Taylor Expansion of the Differential Range for Monostatic SAR

BRIAN D. RIGLING, Student, IEEE

RANDOLPH L. MOSES, Senior Member, IEEE
Ohio State University

The polar format algorithm (PFA) for spotlight synthetic aperture radar (SAR) is based on a linear approximation for the differential range to a scatterer. We derive a second-order Taylor series approximation of the differential range. We provide a simple and concise derivation of both the far-field linear approximation of the differential range, which forms the basis of the PFA, and the corresponding approximation limits based on the second-order terms of the approximation.

Manuscript received July 12, 2002; revised April 28, 2003; released for publication August 19, 2004.

IEEE Log No. T-AES/41/1/844810.

Refereeing of this contribution was handled by P. Lombardo.

Authors' addresses: B. D. Rigling, Dept. of Electrical Engineering, Wright State University, Dayton, OH; R. L. Moses, Dept. of Electrical Engineering, Ohio State University, 2015 Neil Ave., Columbus, OH 43210-1272, E-mail: (moses.2@osu.edu).

I. INTRODUCTION

The polar format algorithm (PFA) [1–3] has long been a mainstay of spotlight synthetic aperture radar (SAR) image formation. The key to the PFA is an approximation commonly known as the far-field assumption. This expression gives a linear estimate for the phase of monostatic SAR phase history data. By interpolating the collected frequency domain data onto a uniformly sampled rectangular grid, the far-field linear approximation allows matched filtering of the sampled phase histories through the use of a two-dimensional discrete Fourier transform (DFT), thus admitting the use of fast Fourier transforms (FFTs) and allowing image formation in $O(N^2 \log_2 N)$ operations.

In the work presented here, we develop a simple, concise derivation of the far-field linear approximation and the associated approximation limits. We describe the monostatic SAR data collection geometry and the quantity, known as differential range, which arises from it. The first-order terms of the Taylor expansion of differential range define the far-field assumption. The limits that this linear approximation imposes on the image scene size are determined by the second-order terms of that same expansion.

Far-field approximations of the differential range have been derived in several works: see e.g., [1–3]. However, in the context of the complex overall topic being addressed, the beauty and simplicity of this derivation is frequently difficult to extract. In addition, the derived far-field assumption is used not only for SAR image formation, but in other applications as well. For example, SAR image exploitation techniques for automatic target recognition often make use of the far-field approximation when describing target chips and full scenes in the phase history domain (i.e., frequency space) [4–7, 9, 10]. We present a simple and concise derivation of the Taylor expansion of the differential range for a monostatic geometry. From this expansion, we state the far-field assumption, and we also derive the scene size limits imposed by this linear phase approximation.

II. MONOSTATIC SAR DATA COLLECTION

We consider the monostatic SAR geometry shown in Fig. 1. A scene to be imaged is centered at the origin of the coordinate system. The combined transmit and receive radar antenna platform moves nominally in the $+y$-direction. The actual path of the antenna platform is $\mathbf{r}_a(\tau) = (x_a(\tau), y_a(\tau), z_a(\tau))$. The antenna platform measures its path while flying, and the error in measuring that path is $\tilde{\mathbf{r}}_a(\tau) = (\tilde{x}_a(\tau), \tilde{y}_a(\tau), \tilde{z}_a(\tau))$. A scatterer in the scene is located at a point $\mathbf{r}_0 = (x, y, z)$, near the scene origin. As the antenna platform moves along its flight path, it periodically transmits pulses of energy in the direction

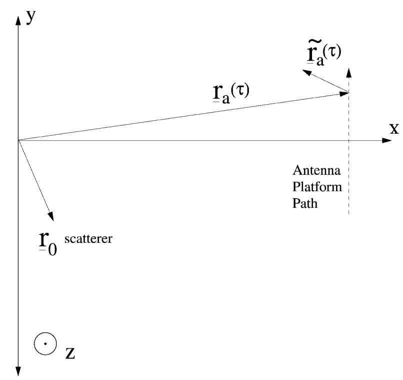

Fig. 1. Top view of x-y ground plane, monostatic SAR geometry.

of the scene center. Each transmitted pulse travels from the transmitter to the scene of interest, where it is reflected by any scatterers within the area of illumination. This reflected energy disperses in all directions, and some of this energy is observed back at the antenna platform. The output of the receiver at a given time τ is assumed to be band-limited frequency domain samples of a pulse delayed by the round-trip time to the target, written as

$$S(f,\tau) = e^{-j2\pi f(2d_{a0}(\tau)/c)} \tag{1}$$

where $d_{a0}(\tau) = \|\mathbf{r}_a(\tau) - \mathbf{r}_0(\tau)\|$ is the distance from the antenna platform to the scatterer. The receiver gates its sampling in the time domain in such a way that a scatterer at the scene center will have zero phase, making the received signal

$$S(f,\tau) = e^{-j2\pi f(2(d_{a0}(\tau)-d_a(\tau))/c)} \tag{2}$$

where $d_a(\tau) = \|\mathbf{r}_a(\tau) + \tilde{\mathbf{r}}_a(\tau)\|$ is the measured distance from the antenna platform to the scene center. The difference between the distances $d_{a0}(\tau)$ and $d_a(\tau)$ is typically referred to as the differential range $\Delta R(\tau)$. We wish to obtain a linear approximation of this quantity for use in the PFA. We then derive the limitations imposed by discarding the higher order terms.

III. TAYLOR EXPANSION OF DIFFERENTIAL RANGE

From (2), the differential range at time τ is

$$\Delta R(\tau) = d_{a0}(\tau) - d_a(\tau) \tag{3}$$

where the distance between the antenna and a scatterer in the scene is

$$d_{a0} = \sqrt{(x_a - x)^2 + (y_a - y)^2 + (z_a - z)^2} \tag{4}$$

and the measured distance to the scene origin is

$$d_a = \sqrt{(x_a + \tilde{x}_a)^2 + (y_a + \tilde{y}_a)^2 + (z_a + \tilde{z}_a)^2}. \tag{5}$$

For the remainder of this derivation, the time variable τ is suppressed. To obtain the Taylor expansion of ΔR, one may expand d_{a0} with respect to the scatterer location about the point $(x,y,z) = (0,0,0)$, and may expand d_a with respect to the measurement error about the point $(\tilde{x}_a,\tilde{y}_a,\tilde{z}_a) = (0,0,0)$. The difference between the constant terms of these expansions is zero, implying $\Delta R^{(0)}$ is zero. The first-order terms of ΔR with respect to the vector $[x,y,z,\tilde{x}_a,\tilde{y}_a,\tilde{z}_a]^T$ are

$$\begin{aligned}\Delta R^{(1)} = {} & \left.\frac{\partial d_{a0}}{\partial x}\right|_{x=0} x + \left.\frac{\partial d_{a0}}{\partial y}\right|_{y=0} y + \left.\frac{\partial d_{a0}}{\partial z}\right|_{z=0} z \\ & - \left.\frac{\partial d_a}{\partial \tilde{x}_a}\right|_{\tilde{x}_a=0} \tilde{x}_a - \left.\frac{\partial d_a}{\partial \tilde{y}_a}\right|_{\tilde{y}_a=0} \tilde{y}_a - \left.\frac{\partial d_a}{\partial \tilde{z}_a}\right|_{\tilde{z}_a=0} \tilde{z}_a\end{aligned} \tag{6}$$

which when evaluated gives

$$\Delta R^{(1)} = \frac{-x_a(x+\tilde{x}_a) - y_a(y+\tilde{y}_a) - z_a(z+\tilde{z}_a)}{\sqrt{x_a^2 + y_a^2 + z_a^2}}. \tag{7}$$

By expressing the antenna location $\mathbf{r}_a = (x_a,y_a,z_a)$ in polar coordinates (r_a,ϕ_a,θ_a), (7) can be used to write the far-field approximation

$$\begin{aligned}\Delta R \approx {} & -(x+\tilde{x}_a)\cos\phi_a\cos\theta_a \\ & -(y+\tilde{y}_a)\sin\phi_a\cos\theta_a - (z+\tilde{z}_a)\sin\theta_a\end{aligned} \tag{8}$$

where $x_a = r_a\cos\phi_a\cos\theta_a$, $y_a = r_a\sin\phi_a\cos\theta_a$, and $z_a = r_a\sin\theta_a$. This estimate for ΔR is used to define the PFA matched filter kernel

$$\begin{aligned}\exp\Bigg[& -j\frac{4\pi f}{c}(x\cos\phi_a(\tau)\cos\theta_a(\tau) + y\sin\phi_a(\tau)\cos\theta_a(\tau) \\ & + z\sin\theta_a(\tau))\Bigg]\end{aligned} \tag{9}$$

where the motion measurement errors have been set to zero, and typically z is also set to zero in order to form a ground plane image.

We next analyze the phase errors introduced by using (9) to form images. To do so we need to find the second-order terms of the Taylor expansion of ΔR. The 6×6 Hessian matrix of ΔR is block diagonal with respect to $[x,y,z,\tilde{x}_a,\tilde{y}_a,\tilde{z}_a]^T$, with the 3×3 off-diagonal blocks equal to zero, thus implying that

$$\Delta R^{(2)} = d_{a0}^{(2)} - d_a^{(2)} \tag{10}$$

where

$$\begin{aligned}d_{a0}^{(2)} = {} & \left.\frac{\partial^2 d_{a0}}{\partial x^2}\right|_{x=0}\frac{x^2}{2} + \left.\frac{\partial^2 d_{a0}}{\partial x\partial y}\right|_{x,y=0}\frac{xy}{2} \\ & + \left.\frac{\partial^2 d_{a0}}{\partial x\partial z}\right|_{x,z=0}\frac{xz}{2} + \left.\frac{\partial^2 d_{a0}}{\partial y^2}\right|_{y=0}\frac{y^2}{2} \\ & + \left.\frac{\partial^2 d_{a0}}{\partial y\partial x}\right|_{y,x=0}\frac{yx}{2} + \left.\frac{\partial^2 d_{a0}}{\partial y\partial z}\right|_{y,z=0}\frac{yz}{2} \\ & + \left.\frac{\partial^2 d_{a0}}{\partial z^2}\right|_{z=0}\frac{z^2}{2} + \left.\frac{\partial^2 d_{a0}}{\partial z\partial x}\right|_{z,x=0}\frac{zx}{2} \\ & + \left.\frac{\partial^2 d_{a0}}{\partial z\partial y}\right|_{z,y=0}\frac{zy}{2}\end{aligned}$$

$$= \frac{x^2}{2}\left(\frac{y_a^2 + z_a^2}{r_a^3}\right) + \frac{y^2}{2}\left(\frac{x_a^2 + z_a^2}{r_a^3}\right) + \frac{z^2}{2}\left(\frac{x_a^2 + y_a^2}{r_a^3}\right) - xy\left(\frac{x_a y_a}{r_a^3}\right) - xz\left(\frac{x_a z_a}{r_a^3}\right) - yz\left(\frac{y_a z_a}{r_a^3}\right) \tag{11}$$

and

$$\begin{aligned} d_a^{(2)} &= \left.\frac{\partial^2 d_a}{\partial \tilde{x}_a^2}\right|_{\tilde{x}_a=0} \frac{\tilde{x}_a^2}{2} + \left.\frac{\partial^2 d_a}{\partial \tilde{x}_a \partial \tilde{y}_a}\right|_{\tilde{x}_a,\tilde{y}_a=0} \frac{\tilde{x}_a \tilde{y}_a}{2} \\ &+ \left.\frac{\partial^2 d_a}{\partial \tilde{x}_a \partial \tilde{z}_a}\right|_{\tilde{x}_a,\tilde{z}_a=0} \frac{\tilde{x}_a \tilde{z}_a}{2} + \left.\frac{\partial^2 d_a}{\partial \tilde{y}_a^2}\right|_{\tilde{y}_a=0} \frac{\tilde{y}_a^2}{2} \\ &+ \left.\frac{\partial^2 d_a}{\partial \tilde{y}_a \partial \tilde{x}_a}\right|_{\tilde{y}_a,\tilde{x}_a=0} \frac{\tilde{y}_a \tilde{x}_a}{2} + \left.\frac{\partial^2 d_a}{\partial \tilde{y}_a \partial \tilde{z}_a}\right|_{\tilde{y}_a,\tilde{z}_a=0} \frac{\tilde{y}_a \tilde{z}_a}{2} \\ &+ \left.\frac{\partial^2 d_a}{\partial \tilde{z}_a^2}\right|_{\tilde{z}_a=0} \frac{\tilde{z}_a^2}{2} + \left.\frac{\partial^2 d_a}{\partial \tilde{z}_a \partial \tilde{x}_a}\right|_{\tilde{z}_a,\tilde{x}_a=0} \frac{\tilde{z}_a \tilde{x}_a}{2} \\ &+ \left.\frac{\partial^2 d_a}{\partial \tilde{z}_a \partial \tilde{y}_a}\right|_{\tilde{z}_a,\tilde{y}_a=0} \frac{\tilde{z}_a \tilde{y}_a}{2} \\ &= \frac{\tilde{x}_a^2}{2}\left(\frac{y_a^2 + z_a^2}{r_a^3}\right) + \frac{\tilde{y}_a^2}{2}\left(\frac{x_a^2 + z_a^2}{r_a^3}\right) + \frac{\tilde{z}_a^2}{2}\left(\frac{x_a^2 + y_a^2}{r_a^3}\right) \\ &- \tilde{x}_a \tilde{y}_a\left(\frac{x_a y_a}{r_a^3}\right) - \tilde{x}_a \tilde{z}_a\left(\frac{x_a z_a}{r_a^3}\right) - \tilde{y}_a \tilde{z}_a\left(\frac{y_a z_a}{r_a^3}\right). \end{aligned} \tag{12}$$

IV. SCENE SIZE LIMITS FOR A MONOSTATIC GEOMETRY

The PFA kernel in (9) is found by neglecting higher order phase terms. The effect of this approximation, typically referred to as the error due to range curvature [1–3], may be characterized by analyzing the second-order terms defined by (10)–(12), which are assumed to be the dominant sources of phase approximation errors [8]. By examining the first neglected terms of the Taylor expansion of ΔR, we remain consistent with the accepted methodology established in [1–3]. Given the similar forms of $d_{a0}^{(2)}$ and $d_a^{(2)}$, one may focus attention on the effects of $d_{a0}^{(2)}$ and draw analagous conclusions with respect to $d_a^{(2)}$.

We must first recall the time dependence of x_a, y_a, and z_a. It was assumed in Section II that the antenna platform travels strictly in the $+y$-direction, such that the x_a and z_a coordinates remain constant across the aperture, while $y_a = v_a\tau$ varies linearly with time. Furthermore, we now assume that r_a is sufficiently large at the aperture center such that r_a may be assumed to be constant with respect to time. By applying these assumptions to (11), it can be seen that $d_{a0}^{(2)}$ is comprised of terms which are constant, linear, and quadratic with respect to slow time τ. The constant and linear terms will introduce spatially dependent distortions in the final image, such that scatterers actually located at (x,y,z) will appear at some (x',y',z'), but do not cause any blurring or loss of resolution. Terms of $d_{a0}^{(2)}$ that are quadratically dependent on time (which are those containing y_a^2) will cause a spatially dependent defocus, or blurring, of scatterers. The approximation limits for the far-field assumption are typically determined by bounding the amount of defocus experienced by scatterers on the ground plane ($z = 0$). With $z = 0$, only the $x^2 y_a^2/(2r_a^3)$ term (with $y_a = v_a\tau$) depends quadratically on τ.

Equation (2) shows that the phase of a received pulse as defined by the differential range is

$$\Phi = -2\pi f \frac{2\Delta R}{c} \tag{13}$$

and thus the defocusing phase error due to range curvature is

$$\Phi_c = -\frac{4\pi f}{c}\frac{1}{2}\frac{x^2 y_a^2}{r_a^3}. \tag{14}$$

One typically prefers to limit this phase error to no more than $\pm\pi/2$ at the maximum extents of the scene $x = \pm r_{\max}$ and the maximum extents of the synthetic aperture $y_a = \pm L_a/2$, where L_a is the length of the synthetic aperture. Limiting the magnitude of the quadratic phase error to be less than $\pi/2$ typically makes the phase errors introduced by the far-field approximation insignificant relative to the errors caused by interpolation errors and residual platform motion measurement errors. Substituting in the length of the synthetic aperture, and the wavelength λ in place of c/f, the inequality $|\Phi_c| < \pi/2$ may be expressed as

$$\frac{\pi}{2} > \frac{\pi}{2\lambda}\frac{r_{\max}^2 L_a^2}{r_a^3}. \tag{15}$$

For the special case of broadside imaging, the cross-range resolution of a SAR is approximately [2]

$$\Delta_y = \frac{r_a \lambda}{2L_a}. \tag{16}$$

The inequality of (15) may therefore be rewritten as

$$\frac{\pi}{2} > \frac{\pi r_{\max}^2 \lambda}{8\Delta_y^2 r_a} \tag{17}$$

which may then be rearranged to give

$$r_{\max} < 2\Delta_y \sqrt{\frac{r_a}{\lambda}} \tag{18}$$

thus limiting the maximum radius of an image formed by the PFA.

An identical restriction may be derived for the approximation limits on $(\tilde{x}_a, \tilde{y}_a, \tilde{z}_a)$. However, as these motion measurement errors are unknown, we have no a priori means by which to limit them. Furthermore, the phase errors introduced by these unknown motion measurement errors will cause irreparable defocus to an image long before the far-field approximation (8) breaks down.

V. CONCLUSIONS

We have described the monostatic SAR data collection geometry and defined the differential range of a scatterer. We then derived the second-order Taylor expansion of the differential range. From this, we highlighted the first-order linear approximation, known as the far-field assumption, which is used to define the matched filtering kernel of the PFA. Finally, we analyzed the phase error introduced by using this linear approximation, and thus determined limits on the maximum size of scene that may be imaged using the PFA.

REFERENCES

[1] Walker, J. L. (1980)
Range-Doppler imaging of rotating objects.
IEEE Transactions on Aerospace and Electronic Systems, **AES-16** (Jan. 1980), 23–52.

[2] Carrara, W. G., Goodman, R. S., and Majewski, R. M. (1995)
Spotlight Synthetic Aperture Radar: Signal Processing Algorithms.
Norwood, MA: Artech House, 1995.

[3] Jakowatz, C. V., Wahl, D. E., and Eichel, P. H. (1996)
Spotlight-Mode Synthetic Aperture Radar: A Signal Processing Approach.
Boston, MA: Kluwer Academic Publishers, 1996.

[4] Potter, L. C., andMoses, R. L. (1997)
Attributed scattering centers for SAR ATR.
IEEE Transactions on Image Processing, **6**, 1 (Jan. 1997), 79–91.

[5] Potter, L. C., Chiang, D-M., Carriere, R., and Gerry, M. J. (1995)
A GTD-based parametric model for radar scattering.
IEEE Transactions on Antennas and Propagation, **43**, 10 (Oct. 1995), 1058–1067.

[6] Bi, Z., Li, J., and Liu, Z. (1999)
Super resolution of SAR imaging via parametric spectral estimation methods.
IEEE Transactions on Aerospace and Electronic Systems, **35**, 1 (Jan. 1999), 267–281.

[7] Chiang, H., Moses, R. L., and Potter, L. C. (2000)
Model-based classification of radar images.
IEEE Transactions on Information Theory, **46**, 5 (Aug. 2000), 1842–1854.

[8] Gerald, C. F., and Wheatley, P. O. (1994)
Applied Numerical Analysis.
Reading, MA: Addison-Wesley, 1994.

[9] Walton, E. K., Chamberlain, N. F., and Garber, F. D. (1991)
Radar target identification of aircraft using polarization-diverse features.
IEEE Transactions on Aerospace and Electronic Systems, **27** (Jan. 1991), 58–67.

[10] Chamberlain, N. F., Garber, F. D., and Snorrason, O. (1988)
Time-domain and frequency-domain feature selection for reliable radar target identification.
In *Proceedings of the IEEE 1988 National Radar Conference*, Apr. 1988, 79–84.

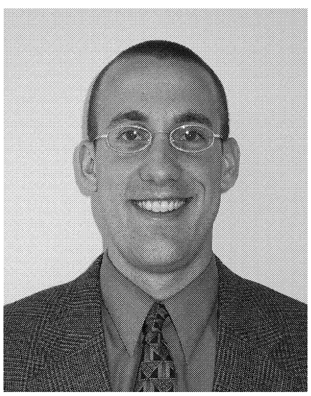

Brian D. Rigling (S'00) received the B.S. degree in physics-computer science from the University of Dayton, Dayton, OH, in 1998 and received the M.S. and Ph.D. degrees in electrical engineering from The Ohio State University, Columbus, in 2000 and 2003, respectively.

Since July 2004 he has been with the Department of Electrical Engineering, Wright State University, and is currently an assistant professor there. From 2000 to 2004 he was a radar systems engineer for Northrop Grumman Electronic Systems in Baltimore, MD. His research interests are in sensor signal processing and system engineering, array processing, autofocus, parametric modeling, and estimation.

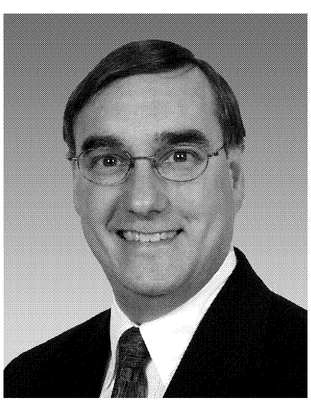

Randolph L. Moses (S'78—M'85—SM'90) received the B.S., M.S., and Ph.D. degrees in electrical engineering from Virginia Polytechnic Institute and State University, Blacksburg, in 1979, 1980, and 1984, respectively.

Since 1985 he has been with the Department of Electrical Engineering, The Ohio State University, and is currently a professor there. During the summer of 1983 he was a summer faculty research fellow at Rome Air Development Center, Rome, NY. From 1984 to 1985 he was a NATO postdoctoral fellow at Eindhoven University of Technology, Eindhoven, The Netherlands. During 1994–1995 he was on sabbatical leave at Uppsala University in Sweden, and in 2002–2003 he was on sabbatical leave at Air Force Research Laboratory in Ohio and at Massachusetts Institute of Technology. His research interests are in stochastic signal processing, and include parametric estimation, array signal processing, sensor networks, and radar imaging.

Dr. Moses served as associate editor for the *IEEE Transactions on Signal Processing* from 2001–2004 and served on the IEEE Signal Processing Society Technical Committee on Statistical Signal and Array Processing from 1991–1994. He is coauthor with P. Stoica of *Introduction to Spectral Analysis* (Prentice Hall, 1997). He is a member of Eta Kappa Nu, Tau Beta Pi, Phi Kappa Phi, and Sigma Xi.